water

Article

The Potential of AOP Pretreatment in the Biodegradation of PS and PVC Microplastics by *Candida parapsilosis*

Kristina Bule Možar [1], Martina Miloloža [1], Viktorija Martinjak [1], Magdalena Ujević Bošnjak [2], Marinko Markić [1], Tomislav Bolanča [1], Matija Cvetnić [1], Dajana Kučić Grgić [1,*] and Šime Ukić [1,*]

[1] Faculty of Chemical Engineering and Technology, University of Zagreb, Trg Marka Marulića 19, 10000 Zagreb, Croatia; kbule@fkit.unizg.hr (K.B.M.); miloloza@fkit.unizg.hr (M.M.); vprevaric@fkit.unizg.hr (V.M.); mmarkic@fkit.unizg.hr (M.M.); tbolanca@fkit.unizg.hr (T.B.); mcvetnic@fkit.unizg.hr (M.C.)

[2] Croatian Institute of Public Health, Rockefellerova 7, 10000 Zagreb, Croatia; magdalena.ujevic@hzjz.hr

* Correspondence: dkucic@fkit.unizg.hr (D.K.G.); sukic@fkit.unizg.hr (Š.U.); Tel.: +385-14597238 (D.K.G.); +385-14597217 (Š.U.)

Abstract: Microplastics are an emerging class of recalcitrant organic pollutants that are of general scientific and public interest nowadays. It would be ideal to remove microplastics from the environment through biodegradation, as biodegradation is a highly ecological and economically acceptable approach. Unfortunately, the efficiency of biodegradation of conventional plastic polymers is low. The application of a suitable pretreatment could increase the efficiency of biodegradation. In this study, the applicability of UV-C/H_2O_2 and UV-C/$S_2O_8^{2-}$ advanced oxidation processes as pretreatments for the biodegradation of polystyrene and poly(vinyl chloride) microplastics by the yeast *Candida parapsilosis* was investigated. For the investigated range (pH 4–10, peroxide concentration up to 20 mM and treatment duration up to 90 min), the UV-C/H_2O_2 process proved to be more effective in degrading polystyrene microplastics, while the UV-C/$S_2O_8^{2-}$ process was more efficient at degrading poly(vinyl chloride) microplastics. Samples pretreated under optimal conditions (90 min treatment time at a pH of 5.7 and H_2O_2 concentration of 20.0 mM for polystyrene samples; 90 min treatment time at a pH of 8.6 and $S_2O_8^{2-}$ concentration of 11.1 mM for poly(vinyl chloride) samples) were subjected to biodegradation by *Candida parapsilosis*. The biodegradation conditions included an agitation speed of 156 rpm and an initial pH of 5.7 for the experiments with the polystyrene samples, while an agitation speed of 136 rpm and an initial pH of 4.9 were used for the poly(vinyl chloride) experiments. The initial value of the optical density of the yeast suspension was 1.0 in both cases. The experiments showed a positive effect of the pretreatment on the number of yeast cells on the surface of the microplastics.

Keywords: microplastics; polystyrene; poly(vinyl chloride); advanced oxidation; UV-C/H_2O_2; UV-C/$S_2O_8^{2-}$

check for updates

Citation: Bule Možar, K.; Miloloža, M.; Martinjak, V.; Ujević Bošnjak, M.; Markić, M.; Bolanča, T.; Cvetnić, M.; Kučić Grgić, D.; Ukić, Š. The Potential of AOP Pretreatment in the Biodegradation of PS and PVC Microplastics by *Candida parapsilosis*. *Water* **2024**, *16*, 1389. https://doi.org/10.3390/w16101389

Academic Editors: Kai He, Jing Wei, Zhishui Liang and Yuanfeng Qi

Received: 5 April 2024
Revised: 3 May 2024
Accepted: 11 May 2024
Published: 13 May 2024

1. Introduction

Plastic is an extremely useful polymer material with incredible application properties [1]. Unfortunately, a large number of plastic products end up in the environment, posing a serious environmental threat [2]. Small plastic particles, known as microplastics (MPs, particles with a size of 1–5000 μm) and nanoplastics (NPs, particles with a size of less than 1 μm), are considered particularly hazardous [3].

The *2030 Agenda for Sustainable Development*, adopted by the United Nations in September 2015 [4], includes 17 Sustainable Development Goals (SDGs), and half of these goals are directly affected by the problem of plastic pollution [5]. As part of SDG 12, *Responsible Consumption and Production*, the agenda promotes a more rational use of raw materials and products. In the context of plastics, this would inevitably lead to less plastic waste entering the environment. Furthermore, it should not be forgotten that the production of conventional plastic polymers (polyethylene, polypropylene, polyethylene terephthalate, polystyrene (PS) and poly(vinyl chloride) (PVC)) is associated with high CO_2 emissions, as these polymers are made from fossil fuels, and their production requires high energy consumption. A reduction in plastic production is therefore linked to SDG *13*, *Climate Action*. The effective collection and processing of plastic waste would be a step towards achieving SDG *11*, *Sustainable Cities and Communities*. Conventional plastic polymers are recalcitrant organic pollutants. The presence of their MPs or NPs in the environment affects the achievement of the SDGs in various ways. MP and NP particles can easily enter the animal/human body due to their small size and cause harmful biological effects [6]. Also, do not forget that MPs serve as vectors for pathogens when adsorbed on their surface [7]. Finally, MP and NP particles from commercially available plastics usually contain various additives, some of which have a high toxic potential. As these additives are not covalently bound, they leach unhindered into the environment [8]. All of this has a direct impact on four SDGs: SDG *3*, *Good Health and Well-being*, *SDG 4*, *Clean Water and Sanitation*, SDG *14*, *Protection of Seas and Oceans* and SDG *15*, *Repair Ecosystems and Retain Biodiversity*.

In recent decades, scientists have been intensively researching methods to effectively remove MPs and NPs from the environment, especially from the aquatic environment. Some of the conventional approaches to remove MPs from aquatic media are adsorption on a suitable adsorbent and coagulation with a suitable coagulant. However, the addition of adsorbents or coagulants can provide a new source of water pollution. Membrane processes are considered to be very successful in the removal of MPs. The problem with membrane processes, however, is the high operating and maintenance costs. All three processes mentioned have a common problem: the sludge produced during treatment. The sludge, which is rich in MPs, must be treated further [9]. However, it is often used untreated on agricultural land, creating another pathway for MPs in the environment [10,11].

Biotreatment is considered the most environmentally and economically acceptable approach to the remediation of polluted environments [12]. Due to their rapid reproduction rate and high metabolic potential, bacteria and fungi are able to adapt to new substrates and are therefore the most studied organisms for the biodegradation of conventional plastic polymers [13]. The pathway for the biochemical degradation of MPs is not uniform and depends on the polymer treated and the characteristics of the enzymatic system of the microorganism used for the treatment. Before the biodegradation of MPs can begin, several general conditions must be met: Firstly, the surface of the MPs must be such that microorganisms can adhere to the surface [14]; this is the basic prerequisite for the formation of a biofilm on the surface of MPs. Secondly, the selected microorganisms must be able to produce extracellular enzymes that can break down the plastic polymer into smaller molecules. Finally, these microorganisms must also be able to utilize these smaller molecules as a carbon source, i.e., as an energy source, with the help of an intracellular enzyme system [15]. However, the conventional plastic polymers are extremely stable substances whose structures do not have functional groups that are frequently attacked by enzymes [16]. In addition, these polymers are hydrophobic [17], which makes it difficult for most bacteria and fungi to adhere to the surface of the plastic particles. Most bacteria have hydrophilic cell membranes [18], as do yeast cells and the vegetative hyphae of filamentous fungi that grow in humid environments [19]. Therefore, conventional plastics are not readily biodegradable [20], which complicates the biological approach to solving the problem of MPs in the environment. Therefore, it seems reasonable to apply some kind of a pretreatment that would facilitate biodegradation.

One of the interesting approaches is the use of advanced oxidation processes (AOPs). AOPs are based on the generation of highly reactive radicals with pronounced oxidative capabilities. Therefore, these radicals are able to oxidize a wide range of recalcitrant organic pollutants [21]. The first step in the radical degradation of MPs is either the abstraction of hydrogen or the scission of the C-C bond, which leads to alkyl radicals on the surface of the MPs. Further oxidation leads to chain branching and scission, resulting in the formation of oxygen-containing groups (hydroxyl, peroxide and carbonyl groups) and microcracks in the polymer surface [22]. Although the effectiveness of AOPs in removing various recalcitrant organic pollutants is well documented, AOPs are generally non-selective treatments that require the significant consumption of chemicals, and very often, the use of electricity, which calls into question their cost effectiveness [23]. It is estimated that the investment costs for these processes are 5 to 20 times higher than for biological processes, while the treatment costs are 3 to 10 times higher [24]. In addition, the intermediate products formed during oxidation pose a potential environmental risk [9]. When using AOPs as a pretreatment for the biodegradation of MPs, the advanced oxidation would only serve to alter the surface of the particles, leading to conditions that facilitate the adhesion of microorganisms to the surface (rougher surface and lower hydrophobicity) or transform the polymer into a form that is more susceptible to biodegradation.

In this study, the potentials of two AOPs as pretreatment steps for the biodegradation of PS and PVC MPs by the yeast *Candida parapsilosis* were investigated. The AOPs investigated in this study included treatment with UV-C-activated hydrogen peroxide (UV-C/H_2O_2) and UV-C-activated peroxodisulfate (UV-C/$S_2O_8{}^{2-}$). These AOPs were selected due to their frequent use in solving problems with recalcitrant organic pollutants and their process characteristics, which are presented below. The efficiencies of the applied pretreatments were evaluated by comparing the intensities of the characteristic bands from the FTIR spectra of the MP samples. The efficiency of the biotreatment step was evaluated by determining the number of colony-forming units.

The UV-C/H_2O_2 process is based on the generation of hydroxyl radicals, HO•, which have a very high standard reduction potential of 2.730 V [25]. The HO• radical is the most studied radical in wastewater treatment, because it is a very reactive, non-selective and ecologically harmless substance with a short lifetime. Furthermore, the rate constants for the reaction between HO• and organic pollutants are in the range of 10^6–10^9 M^{-1} s^{-1} [26], which indicates very rapid oxidation, faster than, for example, when ozone is used for oxidation [27]. During the UV/H_2O_2 process, the photolytic decomposition of each H_2O_2 molecule generates two HO• radicals [28]. H_2O_2 has an absorption maximum at about 254 nm [29,30], which is why UV lamps with a wavelength of 254 nm (UV-C range) are usually used in UV/H_2O_2 processes. In addition to the irradiation wavelength, other factors such as the irradiation intensity, temperature, treatment duration, initial pH of the solution, H_2O_2 dosage, pollutant concentration, matrix, etc., can also influence the efficiency of UV/H_2O_2 treatments [31–34].

The UV/$S_2O_8{}^{2-}$ process is based on the generation of sulfate radicals, $SO_4{\bullet}^-$. Although the $SO_4{\bullet}^-$ radical is a slightly weaker oxidizing agent than the HO• radical, with a standard reduction potential of 2.437 V [25]), the UV/$S_2O_8{}^{2-}$ process offers several advantages over UV/H_2O_2, making it a worthy candidate for solving the problem of recalcitrant organic pollutants in the environment. $SO_4{\bullet}^-$ radicals not only have a high oxidizing power, but also react more selectively by electron transfer with organic compounds containing unsaturated bonds or aromatic π electrons. They efficiently degrade organic compounds within a wider pH range. In addition, the $SO_4{\bullet}^-$ radicals have a half-life of 30–40 µs, which is much longer than 20 ns in the case of HO• radicals [35]. In general, the $SO_4{\bullet}^-$ radicals can be obtained through the physical or chemical activation of peroxodisulfate ($S_2O_8{}^{2-}$) or peroxymonosulfate ($HSO_5{}^-$) [36]. The photoactivation of $S_2O_8{}^{2-}$ leads to two $SO_4{\bullet}^-$ radicals per reactant ion, while in the case of $HSO_5{}^-$, the activation generates one $SO_4{\bullet}^-$ and one HO• radical [37].

The reports on the application of UV/H_2O_2 treatments on PVC MPs are very rare, while the reports on PS MPs are not only rare but also contradictory. Hüffer et al. [38] exposed PS microparticles to a H_2O_2 solution (10% *v*/*v*) under 254 nm light for 96 h and reported no significant change in the specific surface area of the exposed particles. However, Dong et al. [39] also investigated the effect of a UV/H_2O_2 treatment on PS MPs and reported significant changes in the physicochemical properties of the sample. In addition, the UV/H_2O_2 treatment resulted in a reduction in the particle size and especially the contact angle of the MPs. This is encouraging with regard to the potential application of this treatment as a pre-step to biotreatment. Hankett et al. [40] investigated the degradation of the plasticizer bis-2-ethylhexyl phthalate (DEHP) in PVC samples using a UV-C/H_2O_2 treatment; the wavelength of irradiation was 254 nm. In addition to the degradation of the plasticizer, they reported radical chain scission reactions with PVC. This scientific team also found that UV-C irradiation not only plays a role in the production of HO● radicals but can also induce molecular changes on the surface of such plasticized PVC samples, leading to increased surface hydrophilicity with an increasing irradiation time [41]. Similar to the UV/H_2O_2 process, there are very few reports on the use of $S_2O_8^{2-}$-based AOPs to treat PS and PVC MPs. Liu et al. [42] investigated the effects of thermally activated $S_2O_8^{2-}$ treatment on PS microparticles and reported a reduction in the particle size, the formation of holes and cracks on the particle surface and a reduction in the contact angle. Zhang et al. [43] investigated the effect of an $S_2O_8^{2-}$-based AOP on the floatability of MPs from various plastic polymers to utilize floatability as a separation method for MP waste. The MPs treated included PVC and PS particles. We did not find any explicit information about the activation method but assume that it was also a thermal activation. The analysis revealed damage to the surface of the plastic particles, followed by the formation of new groups. At optimal conditions of 0.2 M $S_2O_8^{2-}$, pH 10, 70 °C and a treatment time of 30 min, the contact angles of PVC and PS particles decreased by 0.13° and 12.20°, respectively, indicating an increased hydrophilicity of the MP surface.

To date, studies on the biodegradation of MPs from conventional plastics have mainly focused on bacteria [16]. More recently, researchers have also turned their attention to other microorganisms, in particular fungi [13]. Similar to bacteria, fungi also produce different types of enzymes [44], which makes them very interesting organisms for testing. Compared to bacteria, however, fungi have interesting peculiarities. For example, they have a much higher metabolic rate [45], and filamentous fungi can secrete specific proteins, so-called hydrophobins, which facilitate the adhesion of their hyphae to hydrophobic surfaces [46]. Regarding the biodegradation of PS MPs by fungi, we found, in one of our previous studies [47], that the yeast *Candida parapsilosis* has the potential to degrade PS and PVC MPs. As far as we know, there are no other reports in the literature on the treatment of PS MPs with yeasts, but only with molds and white-rot fungi [48–55]. Regarding the biodegradation of PVC MPs by fungi, biodegradation by yeasts has not been sufficiently investigated yet; the available studies mostly contain experiments with other fungal species [56–60]. Apart from the report of our working group [51], we did not find any reports on biodegradation by *Candida parapsilosis*. However, we found a report by Webb et al. [61]. They exposed a 0.5 mm thick PVC film to the environment and found that after 95 weeks of exposure, only fungi colonized the PVC. Not a single bacterium was found in the biofilm, indicating that fungi have a greater potential to colonize and biodegrade PVC. Among the fungi isolated from the biofilm, numerous yeasts and yeast-like fungi such as *Rhodotorula aurantiaca*, *Kluyveromyces* spp. and *Aureobasidium pullulans* were found, pointing to their ability to adapt to PVC MPs.

Although AOP pretreatment prior to biodegradation is not a new concept in environmental engineering, the studies on the contribution of AOP pretreatment to MP biodegradation are very rare and mainly focused on the contribution of plasma treatment or UV irradiation in the presence of atmospheric air [62–65]. Moreover, as far as we know, this is the first such study on MPs from PS or PVC. Considering that the biodegradation of MPs by yeasts has not yet been sufficiently studied, especially when considering the application of the species *Candida parapsilosis*, it is clear that this research represents an exceptional novelty.

2. Materials and Methods

2.1. Reagents and Solutions

The polymers PS and PVC were purchased as the granules DOKI® POLISTIREN 472 (Dioki d.d., Zagreb, Croatia) and GS-28 (Drvoplast d.d., Buzet, Croatia), respectively. A 30% H_2O_2 solution (p.a.; Gram-Mol d.o.o., Zagreb, Croatia) and solid $Na_2S_2O_8$ (p.a.;

Sigma Aldrich, St. Louis, MO, USA) were used as oxidizing agents in the AOP treatments. Also, 0.04 M H_2SO_4, 0.1 M H_2SO_4 and 0.1 M NaOH were used to adjust the pH of the reaction mixture. The H_2SO_4 solutions were prepared from a 98% H_2SO_4 solution (p.a.; Kemika, Zagreb, Croatia), while the NaOH solution was prepared from solid NaOH (p.a.; Sigma Aldrich, St. Louis, MO, USA). A 2% sodium dodecyl sulfate solution and 70% ethanol solution intended for washing the MP samples after biotreatment were prepared from sodium dodecyl sulfate salt ($\geq$99.0%; Sigma Aldrich, St. Louis, MO, USA) and 96% ethanol (Ph. Eur.; Gram-Mol, Zagreb, Croatia), respectively. Sterile ultrapure water (18.2 $M\Omega$ cm; Milli-Q^{TM} system with UV lamp, Millipore, Burlington, MA, USA) was used for the experiments.

2.2. Preparation and Characterization of Microplastics

The purchased PS and PVC granules were ground in a cryomill (CryoMill, Retsch, Haan, Germany) with liquid nitrogen at −196 °C and an oscillation frequency of 25 Hz. The ground particles were dried at room temperature (25.0 ± 0.2 °C) for 48 h and then sieved through stainless steel sieves (AS 200 jet, Retsch, Haan, Germany) to obtain MPs in the size range of 25–100 µm. The MPs were then stored in glass bottles until used in the experiments.

An FTIR spectrometer (FTIR-8400S, Shimadzu, Kyoto, Japan) with ATR sampling (MIRacle™ Single Reflection ATR, PIKE Technologies, Fitchburg, WI, USA) was used to characterize the MP particles before and after the treatments.

Prior to the biodegradation experiments, MP particles were sterilized for 10 min in a 100 mL flask containing 70% ethanol; the flask was shaken on a rotary shaker (Incubator 1000 equipped with the platform shaker Unimax 1010, Heidolph Instruments, Schwabach, Germany) at 160 rpm. The sterilized particles were separated from the ethanol using vacuum membrane filtration through a sterile 0.45 µm cellulose nitrate filter (ReliaDisc^{TM} membrane filter, Ahlstrom-Munksjö, Helsinki, Finland).

2.3. AOP Treatments

Two homogeneous AOPs, UV/H_2O_2 and UV/$S_2O_8^{2-}$, were tested for the degradation of PS and PVC MPs. The experimental design used for the AOP experiments is shown in Table 1. In the experiments, the influences of three process parameters were tested: the treatment duration, the initial pH value of the reaction mixture and the initial concentration of peroxide. The experiments were designed according to the full factorial methodology, with each variable (i.e., the process parameter) tested at three levels. The mass of MPs was 55.0 mg in all AOP experiments.

Table 1. Experimental design for UV-C/H_2O_2 and UV-C/$S_2O_8^{2-}$; the design combines values for the duration of the treatment (t), the initial pH value of the reaction mixture and the initial concentration of peroxide (c).

No.	*t*/min	pH	*c*/mM	No.	*t*/min	pH	*c*/mM	No.	*t*/min	pH	*c*/mM
1	30	4.0	1.0	10	60	4.0	1.0	19	90	4.0	1.0
2	30	4.0	10.5	11	60	4.0	10.5	20	90	4.0	10.5
3	30	4.0	20.0	12	60	4.0	20.0	21	90	4.0	20.0
4	30	7.0	1.0	13	60	7.0	1.0	22	90	7.0	1.0
5	30	7.0	10.5	14	60	7.0	10.5	23	90	7.0	10.5
6	30	7.0	20.0	15	60	7.0	20.0	24	90	7.0	20.0
7	30	10.0	1.0	16	60	10.0	1.0	25	90	10.0	1.0
8	30	10.0	10.5	17	60	10.0	10.5	26	90	10.0	10.5
9	30	10.0	20.0	18	60	10.0	20.0	27	90	10.0	20.0

The experimental procedure was similar for both AOP treatments. First, 55 mg of an MP sample and 80 mL of water were added to the reactor. The pH was then adjusted to the desired value with 0.04 M H_2SO_4, 0.1 M H_2SO_4 or 0.1 M NaOH. The treatment began with the addition of an appropriate amount of peroxide to the reactor to reach the initial concentration specified in the experimental design (Table 1). The peroxide added was H_2O_2 or $Na_2S_2O_8$, depending on the treatment. During the treatment, the reaction mixture was irradiated at 254 nm (UV-C range) with a mercury lamp (Pen-Ray$^{®}$ 11SC-1, UVP, Upland, CA, USA). The homogeneity of the mixture was maintained by mixing at 150 rpm with a high-speed magnetic stirrer (MS-3000, Biosan, Riga, Latvia). The duration of treatment was varied according to the experimental design (Table 1). The treated samples were separated from the reaction mixture using vacuum filtration through a 0.45 μm cellulose nitrate membrane filter (ReliaDisc^{TM}, Ahlstrom-Munksjö, Helsinki, Finland), washed with water and dried in air for 24 h. The samples were then analyzed using FTIR-ATR.

Analysis of Influential Parameters and Process Optimization

In order to analyze the influence of the selected process parameters on the treatment efficiency and to determine the optimal process conditions, we decided to develop and apply an empirical mathematical model that describes the dependency between the process parameters and the treatment efficiency based on the Response Surface Methodology (RSM).

In a first step, the procedure involved the development of four mathematical models of different complexities. These models, represented by Equations (1)–(4), linearly combine different contributions of three tested process parameters.

$$y = a_0 + a_1x_1 + a_2x_2 + a_3x_3 \tag{1}$$

$$y = a_0 + a_1x_1 + a_2x_2 + a_3x_3 + a_4x_1x_2 + a_5x_1x_3 + a_6x_2x_3 \tag{2}$$

$$y = a_0 + a_1x_1 + a_2x_2 + a_3x_3 + a_7{x_1}^2 + a_8{x_2}^2 + a_9{x_3}^2 \tag{3}$$

$$y = a_0 + a_1x_1 + a_2x_2 + a_3x_3 + a_4x_1x_2 + a_5x_1x_3 + a_6x_2x_3 + a_7{x_1}^2 + a_8{x_2}^2 + a_9{x_3}^2 \tag{4}$$

To simplify the following discussion, we refer to these models with the Roman numerals I to IV. The coefficients of the models are labeled a, while the tested process parameters are labeled x. Model I represents a simple combination of the linear contributions of the tested process parameters. Model II and Model III are extended by interaction and quadratic terms, respectively. Model IV is the most complex of the models used, as it contains all the aforementioned contributions. We decided not to use more complex models, because the first and second order polynomials are the most commonly used in practice, and introducing additional elements into the RSM model would require an experimental design with a much higher number of experimental cases.

The relative change in intensity (CI) of a selected characteristic FTIR peak, calculated according to Equation (5), was used as an indicator of the degradation of MPs, i.e., as the dependent variable y in the RSM models (Equations (1)–(4)).

$$CI = \frac{A_0 - A}{A_0} \cdot 100\% \tag{5}$$

A_0 is the area under the characteristic FTIR band from the spectrum of the untreated sample, and A is the area under the same band from the spectrum of the treated sample. The intensities of the characteristic bands at 694.4 cm^{-1} (out-of-plane C-H bending vibration) [66] and 1411.9 cm^{-1} (CH_2 bending) [67] were determined for PS and PVC samples, respectively.

The second step of the procedure was to analyze the developed models and select the best model for each of the tested MPs-AOP combinations. These best models were used to determine the optimal values of the process parameters based on the location of the maximum of the response surfaces.

Model development and a statistical analysis of the RSM models were performed using MATLAB R2010b software (The MathWorks, Inc., Natick, MA, USA). Optimizations of the parameters for MP treatments were performed using an interactive interface (MATLAB

Response Surface Modeling Tool; *rstool* command). All calculations were performed with 95% confidence.

2.4. Biodegradation Experiments

The biodegradation experiments were performed on PS and PVC samples that had previously been treated under optimal AOP conditions.

The yeast *Candida parapsilosis* was selected for the biodegradation experiments. The yeast was isolated from an MP-rich environment and cultivated as described in detail in one of our previous reports [47]. It is expected that microorganisms inhabiting an MP-rich environment are already adapted to MPs and that they are more efficient in biodegrading plastic polymers than microorganisms that avoid such environments. The same report [47] shows that *Candida parapsilosis* has the highest potential for biodegrading PS and PVC MPs compared to other yeast cultures isolated from the same environment. The biodegradation experiments were carried out under conditions described as optimal in the same report. These included an agitation speed of 156 rpm and an initial pH of 5.7 for experiments with PS samples, while an agitation speed of 136 rpm and an initial pH of 4.9 were used for experiments with PVC samples. The initial value of the number of colony-forming units per mL (CFU) was in the order of 10^7 in all experiments (corresponding to an optical density value of 1.0).

Each biodegradation experiment was performed in an Erlenmeyer flask (200 mL) that was placed in a thermostatic rotary shaker (Incubator 1000 with Unimax 1010 platform shaker, Heidolph Instruments, Schwabach, Germany) at 25.0 ± 0.2 °C for 30 days. The flask contained a mineral medium, the suspension of yeast *Candida parapsilosis* with an optical density of 1.0 and 40 mg of a pretreated MP sample, giving a total working volume of 80 mL; the initial concentration of MPs in the tested system was therefore 500 mg L^{-1}. The mineral medium was prepared according to Gong et al. [68] and contained 1.000 g L^{-1} K_2HPO_4, 1.000 g L^{-1} KH_2PO_4, 1.000 g L^{-1} NH_4NO_3, 0.500 g L^{-1} NaCl, 0.200 g L^{-1} $MgSO_4{\cdot}7H_2O$, 0.020 g L^{-1} $CaCl_2$ and 0.005 g L^{-1} $FeCl_3{\cdot}6H_2O$. A control flask with the mineral medium, the yeast suspension, but without MPs was prepared for a blank experiment. All experiments were performed in duplicate. At the end of each experiment, the treated MP samples were separated from the aqueous phase using vacuum membrane filtration (0.45 µm filter, ReliaDisc^{TM}, Ahlstrom-Munksjö, Helsinki, Finland) and washed in three washing steps to remove the biomass from the surface of the MPs. The steps included washing in 2% sodium dodecyl sulfate solution, 70% ethanol and sterile water, respectively. Each washing step lasted 30 min and was performed in a 100 mL flask on a rotary shaker (Incubator 1000 with Unimax 1010 platform shaker, Heidolph Instruments, Schwabach, Germany) at 160 rpm.

The CFU value was determined on days 0, 3, 7, 14, 21 and 30 to monitor the growth of *Candida parapsilosis*. The CFU values were determined using the decimal plate method [69].

3. Results and Discussion

To characterize the untreated MP samples, an FTIR-ATR analysis of the samples was performed. Figure S1 shows the recorded FTIR spectra, with distinct bands characteristic for the polymers PS and PVC. In the case of PVC, a strong band at 1720.6 cm^{-1} is observed, indicating an additive in the polymer mass, as the strong band in the range of 1700–1725 cm^{-1} corresponds to the C=O stretching of the carboxylic acids [70], while the PVC structure does not contain such groups.

To evaluate the degradation of MPs, we had to select a characteristic FTIR band whose intensity could be monitored. The selection was made among the three most intense bands from the spectra of the untreated PS and PVC samples (Figure S1). These three bands were the C-H bending bands at 694.4 cm^{-1} and 748.4 cm^{-1} and the aromatic C=C stretching band at 1405.5 cm^{-1} in the PS spectrum (Figure S1, case A), while in the PVC spectrum (Figure S1, case B), they were the C-Cl stretching band at 871.8 cm^{-1}, the C-H bending band at 1280.8 cm^{-1} and the CH_2 bending band at 1411.9 cm^{-1}. A general decrease in the intensities of all three bands from the PS spectra was observed during the AOP treatments. A correlation analysis (Table 2) revealed a high positive correlation between these three PS bands, confirming the existence of similar trends in the decrease of band intensities and showing us that fairly similar results are to be expected regardless of which of these three bands are selected. However, to minimize the influence of random error, we selected the band at 694.4 cm^{-1} to monitor PS degradation, because it has the highest initial intensity. For the PVC samples, the correlation analysis revealed a high positive correlation between the intensities of CH_2 bending and C-Cl stretching, while the behavior of the C-H bending band differed from the other two. It should be noted that a general decrease in the intensities of CH_2 bending and C-Cl stretching was observed in both AOP treatments, while the intensity of the C-H band did not seem to be significantly affected by the treatments. Finally, we followed the same logic as for the PS samples and selected the band with the highest initial intensity, where a decrease in the intensity was evident. In the case of the PVC samples, this was the CH_2 band at 1411.9 cm^{-1}.

Table 2. The results of the correlation analysis of the intensities of the three most intense FTIR bands during AOP treatments of PS and PVC MPs. The analysis was performed with a significance of $p < 0.050$.

		PS				**PVC**		
AOP		**694.4 cm^{-1}**	**748.4 cm^{-1}**	**1450.5 cm^{-1}**		**871.8 cm^{-1}**	**1280.8 cm^{-1}**	**1411.9 cm^{-1}**
UV-C/H_2O_2	694.4 cm^{-1}	1.0000			871.8 cm^{-1}	1.0000		
	748.4 cm^{-1}	0.9201	1.0000		1280.8 cm^{-1}	−0.0794	1.0000	
	1405.5 cm^{-1}	0.8352	0.9410	1.0000	1411.9 cm^{-1}	0.9860	−0.0723	1.0000
UV-C/$S_2O_8{}^{2-}$	694.4 cm^{-1}	1.0000			871.8 cm^{-1}	1.0000		
	748.43 cm^{-1}	0.9672	1.0000		1280.8 cm^{-1}	0.4849	1.0000	
	1405.5 cm^{-1}	0.9252	0.9540	1.0000	1411.9 cm^{-1}	0.9372	0.5454	1.0000

The analysis of the applicability of the selected AOPs in the degradation of PS and PVC MPs started with the analysis of the influence of the initial pH of the media, the initial concentration of peroxide and the treatment time on the efficiency of the AOPs.

In the case of the UV-C/H_2O_2 AOP, the influence of the pH of the system reflects, in fact, that the reduction potential of the HO•/H_2O system is pH-dependent. Considering the amount of H_2O_2 added, an increase in the H_2O_2 concentration should increase the formation of HO• radicals and consequently improve the degradation of pollutants. However, an excess of H_2O_2 can decrease the oxidation rate due to scavenging side reactions (Equations (6)–(8)).

$$HO\bullet + H_2O_2 \rightleftarrows HO_2\bullet + H_2O \tag{6}$$

$$2HO_2\bullet \rightleftarrows H_2O_2 + O_2 \tag{7}$$

$$HO\bullet + HO_2\bullet \rightleftarrows H_2O + O_2 \tag{8}$$

The perhydroxyl radicals, $HO_2\bullet$, formed in these reactions have a significantly lower oxidizing power than HO• radicals, since the standard reduction potential of the $HO_2\bullet/H_2O_2$ system is only 1.46 V [25]. In the UV-C/$S_2O_8{}^{2-}$ AOP, the reduction potential of the $SO_4\bullet^-/SO_4{}^{2-}$ system is pH-independent, which means that the pH value should have no influence on the process efficiency. However, the $SO_4\bullet^-$ radical shows a certain degree of autocatalytic behavior, which is most pronounced in the neutral pH range and is suppressed in highly acidic or alkaline solutions [71]. Excessive concentrations of $S_2O_8{}^{2-}$ can lead to a scavenging effect, as shown in Equations (9) and (10) [72].

$$S_2O_8^{2-} + SO_4^{-}\bullet \rightleftarrows SO_2^{2-} + S_2O_8^{-}\bullet \tag{9}$$

$$2SO_4^{-}\bullet \rightleftarrows S_2O_8^{2-} \tag{10}$$

The analysis of the influence of the initial pH of the media, the initial concentration of peroxide and the treatment time required an appropriate mathematical description of the relationship between these process parameters and the relative decrease in intensity of the selected FTIR bands (i.e., the *CI* value). Therefore, a regression diagnosis of four models given by Equations (1)–(4) was first performed. The results of the diagnosis (Table S1) show the significance of all four models, regardless of the MPs and AOP treatments used, as the *p*-value for each of the models is below the applied significance level of 0.050.

Model I is the simplest of the models examined. The results (Table S1) show that the extension of Model I by interaction terms (Model II) or quadratic terms (Model III) led to a better fit of the *CI* values in most cases. This is reflected by an increase in the values of the coefficient of determination (R^2) or the adjusted coefficient of determination (R^2_{adj}). It is important to note that R^2 is not an ideal indicator of which model is better when comparing models with unequal degrees of freedom. The reason for this is that the R^2 increases with each new independent variable that is added to the model, regardless of whether the added variable is relevant or irrelevant for explaining the variation in the dependent variable [73]. To assess the suitability of the model, we therefore compared the values of R^2_{adj}. R^2_{adj} is the value of the coefficient of determination corrected for the number of predictors used in the model. The protection provided by R^2_{adj} is crucial, as too many terms in a regression model can lead to an "over-fitted" model that provides an incorrect description of the system behavior [73]. The comparison of R^2_{adj} values showed that in three situations (both treatments of the PS samples and the PVC sample treated with UV-C/H_2O_2), the introduction of quadratic terms improved the fit of the *CI* values more than the introduction of interaction terms, indicating the greater importance of the quadratic terms in describing the behavior of these systems. Moreover, the introduction of interaction terms in the case of PS MPs treated with UV-C/$S_2O_8{}^{2-}$ even decreased the R^2_{adj} value compared to Model I. On the other hand, the contribution of interaction terms proved to be more beneficial in the case of PVC MPs treated with the UV-C/$S_2O_8{}^{2-}$ process. Finally, Model IV proved to be better than the other three models based on the R^2_{adj} values for all applied AOP treatments, regardless of whether PS or PVC MPs were used. Therefore, this model was used to optimize the AOP treatments.

The estimated values of the coefficients of the RSM models selected as optimal for the applied AOP treatments are presented together with the *t*-test statistics in Table S2, while the graphical representation of each model's response and the determined optimal values of the process parameters can be seen in Figures 1 and 2.

Since the regression analysis was conducted with a significance of 0.05, and the number of degrees of freedom for the selected RSM models was 17, the corresponding critical value for the two-tailed *t*-test was 2.110 [74]. The comparison of the *t*-values for each RSM term with the critical *t*-value (*t*-value above the critical value indicates a significant variable) or analysis of the corresponding *p*-values (*p*-value below the applied significance of 0.05 indicates a significant variable) shows that all three parameters tested—the treatment duration, concentration of peroxide added and pH of the reaction mixture—have a significant influence on the efficacy of the applied AOP treatments. The duration of the AOP treatment does not show a quadratic relation with the *CI* values in any of the cases examined (all *p*-values for the a_7 coefficients are above 0.050). In the case of PS MPs, the contribution of the duration is purely linear regardless of the AOP treatment applied; the significance of the duration is only reflected in the coefficient a_1 ($p < 0.050$). Positive values of this coefficient indicate a positive effect of the treatment extension. For PVC treated with UV-C/H_2O_2, the contribution of the duration is reflected by the linear term (coefficient a_1) and in combination with the pH (a_5), whereas for PVC treated with UV-C/$S_2O_8{}^{2-}$, it is only reflected by the interaction with the concentration of peroxide added (a_4). The coefficients of these interaction terms have a negative sign, which indicates an unfavorable effect of the mutual increase in the values of these process parameters. A linear trend related to the treatment duration, which is visible in the graphical representation of the optimization of the UV-C/$S_2O_8{}^{2-}$ treatment of PVC MPs (Figure 2, case B2), is obviously not specific to the entire experimental area or statistically insignificant. The influence of the linear contribution of the concentration of peroxide proved to be significant in all four cases investigated ($a_2 < 0.050$). In addition, the significance of the quadratic contribution (a_8) was shown in the case of PVC MPs, regardless of the AOP treatment applied. Negative values of the coefficient a_8 indicate a convex dependence, which is unfavorably influenced by too high or too low of an addition of peroxide. The significance of the quadratic term could not be confirmed for the PS samples. Furthermore, in the PS MPs treated with UV-C/H_2O_2, we observed a significant negative influence of the mutual increase in the concentration of peroxide and the pH of the medium ($a_6 < 0.050$), while in the PVC MPs treated with UV-C/$S_2O_8^{2-}$, a significant negative influence of the mutual increase in the concentration of peroxide and the duration of the treatment was observed ($a_4 < 0.050$). In all four cases examined, the importance of the pH value of the medium is initially reflected in the significance of the linear term (a_3) and the quadratic term (a_9). In the case of the UV-C/H_2O_2 treatment, the importance of pH is also reflected in the interaction terms, which show a combined effect with the concentration of peroxide added in the case of PS MPs (coefficient a_6) or with the treatment duration in the case of PVC MPs (coefficient a_5). The negative sign of coefficient a_9, obtained for all four cases examined, indicates the convex character of the pH influence, which is potentially unfavorable when approaching areas with a higher acidity and basicity.

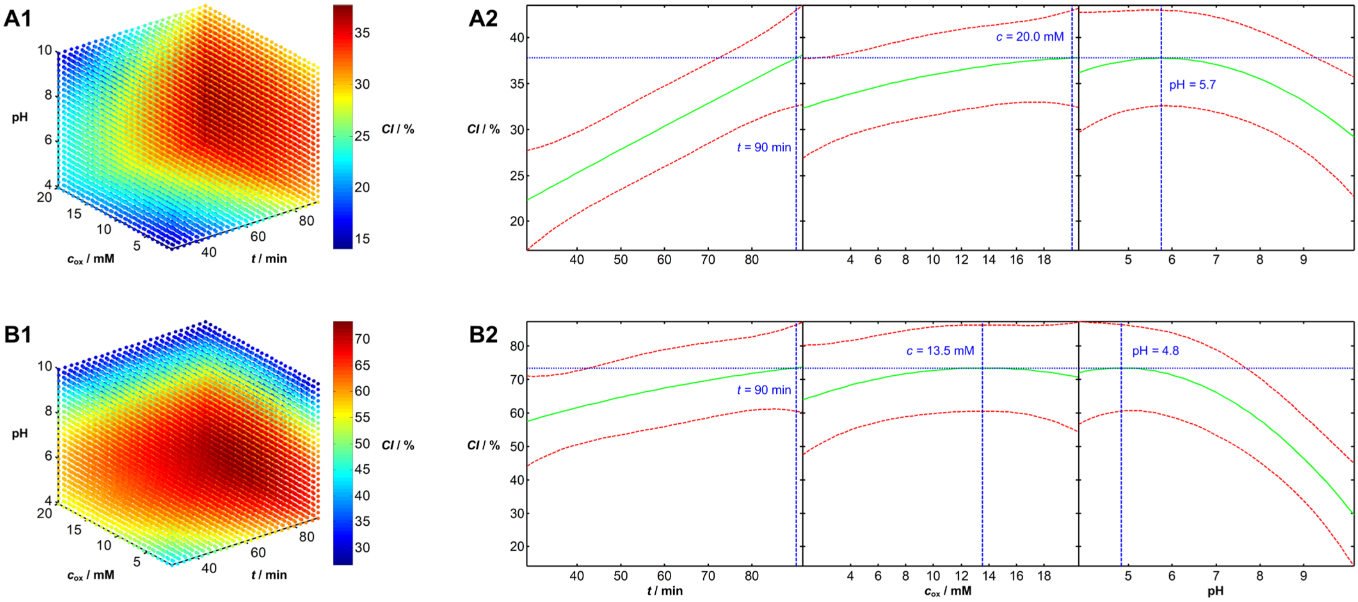

Figure 1. Optimization of UV-C/H_2O_2 treatment of PS MPs (labeled with **A1** and **A2**) and PVC MPs (labeled with **B1** and **B2**). The diagrams under number 1 describe the influence of the process parameters on the treatment efficiency: the response surface is represented with different coloring as the fourth dimension. The diagrams under number 2 show the determination of the optimal process conditions (blue color) by the interactive RSM interface of the MATLAB software: the green line represents the intersection of the response surface, while the red dashed lines are the boundaries of the 95% confidence interval.

The graphical representations of the response surfaces obtained using optimal RSM models are shown in 4D mode (Figures 1 and 2, cases A1 and B1), where the fourth dimension is realized with different coloring: colder colors indicate areas with lower *CI* values, while warmer colors indicate areas with higher *CI* values. The optimal values of the process parameters were determined with 95% confidence using MATLAB's interactive RSM interface and are highlighted in blue in Figures 1 and 2, cases A2 and B2. It can be seen that the experiments with PVC MPs generally resulted in higher *CI* values. Furthermore, the UV-C/H_2O_2 treatment proved to be slightly more effective than the UV-C/$S_2O_8^{2-}$

treatment for the PS samples, while the opposite was true for the PVC samples. As we had previously assumed based on the values of the coefficients of the significant RSM terms, the surface maximum for all four MP-AOP combinations was reached at the longest duration (90 min). The optimum concentration of peroxide was in the high range for PS samples (20.0 mM and 16.8 mM for the UV-C/H_2O_2 treatment and the UV-C/$S_2O_8^{2-}$ treatment, respectively) and in the medium range for PVC samples (13.5 mM and 11.1 mM for the UV-C/H_2O_2 treatment and the UV-C/$S_2O_8^{2-}$ treatment, respectively). Optimum $S_2O_8^{2-}$ concentration values that are below the maximum applied concentration values might result from a scavenging effect according to Equations (9) and (10). The analysis of the influence of the pH showed a favorable effect of a slightly acidic environment for the UV-C/H_2O_2 treatment (optimum pH of 5.7 and 4.8 for PS and PVC samples, respectively) and a neutral to slightly basic environment for the UV-C/$S_2O_8^{2-}$ treatment (optimum pH of 7.4 and 8.6 for PS and PVC samples, respectively). The determined optimal pH values in the case of UV-C/$S_2O_8^{2-}$ treatment might be related to the autocatalytic activity of $SO_4\bullet^-$, which is most pronounced in the neutral pH range [71].

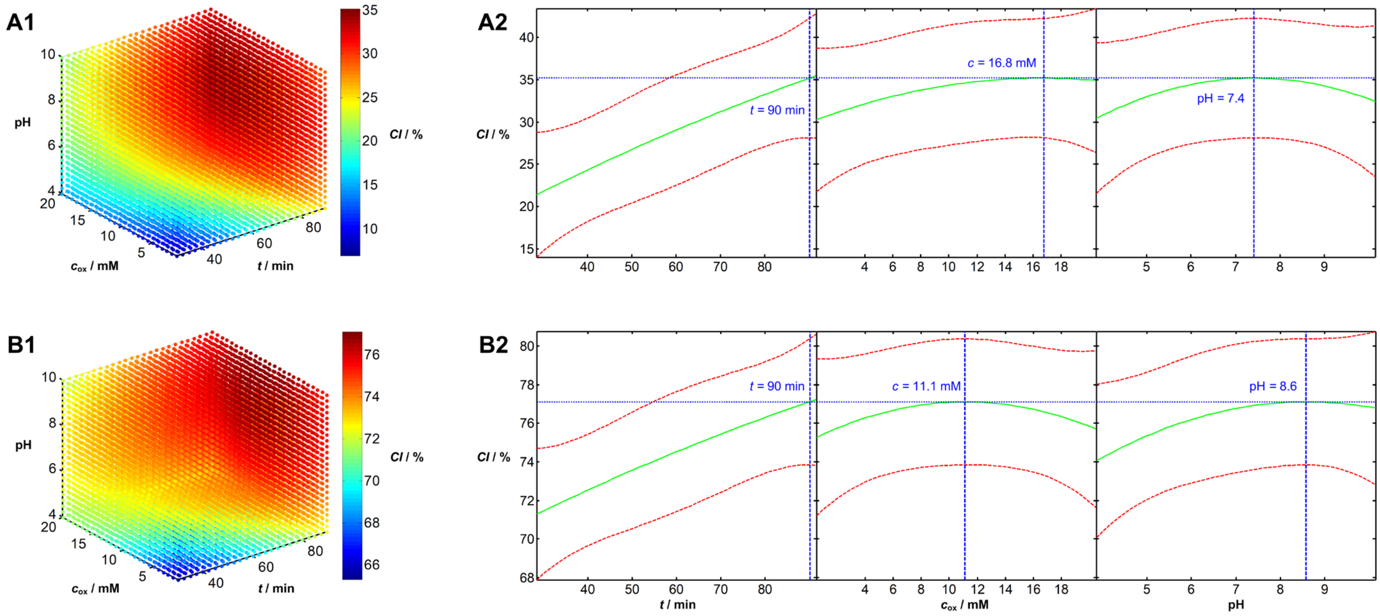

Figure 2. Optimization of UV-C/$S_2O_8^{2-}$ treatment of PS MPs (labeled with **A1** and **A2**) and PVC MPs (labeled with **B1** and **B2**). The diagrams under number 1 describe the influence of the process parameters on the treatment efficiency: the response surface is represented with different coloring as the fourth dimension. The diagrams under number 2 show the determination of the optimal process conditions (blue color) by the interactive RSM interface of the MATLAB software: the green line represents the intersection of the response surface, while the red dashed lines are the boundaries of the 95% confidence interval.

In the following phase of this study, *Candida parapsilosis* was used to biologically treat the pretreated MPs samples. These included PS samples subjected to the UV-C/H_2O_2 pretreatment and PVC samples subjected to the UV-C/$S_2O_8^{2-}$ pretreatment. The AOP pretreatments were carried out under the optimum conditions determined (Figures 1 and 2, cases A2 and B2). Once the biotreatment of the pretreated PS and PVC samples was completed, the samples were analyzed using FTIR-ATR, and the obtained spectra were compared with the spectra of the untreated and pretreated samples (Figure 3).

The blue line in Figure 3 shows a decrease in the intensity of the monitored FTIR band due to pretreatment, which, as mentioned above, is much more pronounced in the case of PVC. An additional decrease in the intensity of the monitored band (red line) due to biodegradation by *Candida parapsilosis* can also be observed for both PS and PVC samples. However, these findings do not indicate whether the AOP pretreatment contributed to the effectiveness of the biodegradation process. To obtain this information, we compared the CFU values obtained during the biotreatment experiments with pretreated MP samples with the CFU values obtained during the experiments with non-pretreated MP samples (Figure 4). The compared CFU values were corrected for the CFU values of the control experiments. Cases A and B in Figure 4 clearly show that the adaptation of the yeast culture to the conditions in the system took place within the first 3 days and that the number of yeast cells remained practically constant thereafter. An exception is the experiment with the non-pretreated PS sample, where a slight descending trend in the CFU values can be observed, indicating that the yeast culture is unable to adapt to this sample and utilize it as a carbon and energy source. It can also be seen that the CFU levels are generally higher in the pretreated samples, regardless of whether they are PS or PVC samples, suggesting that the changes caused by AOP pretreatment made the MP samples more acceptable for *Candida parapsilosis* survival.

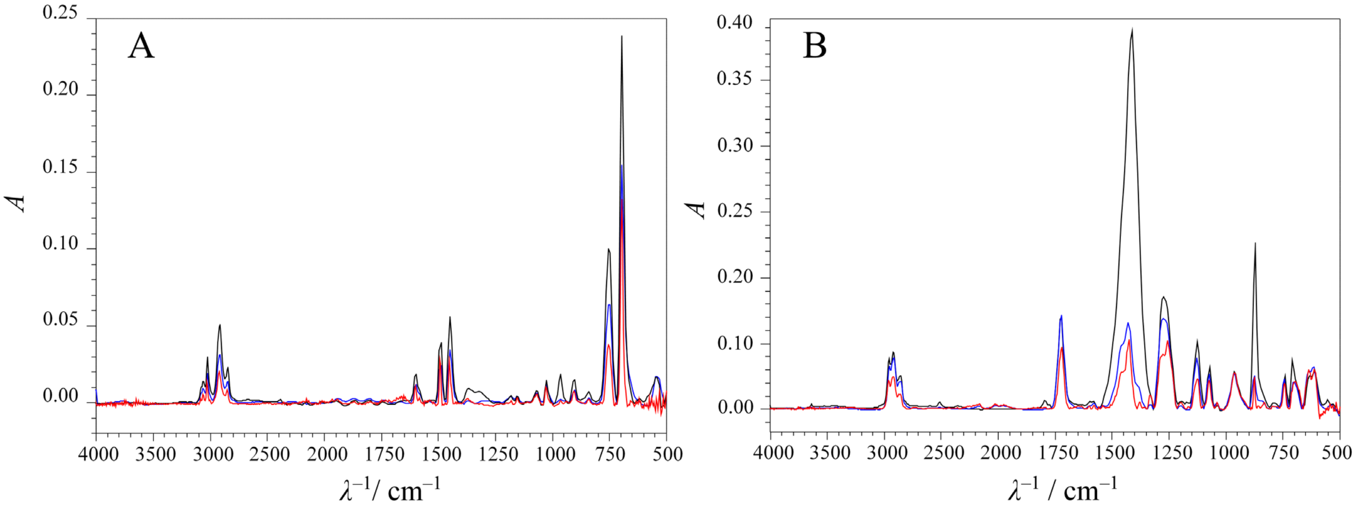

Figure 3. Comparison of FTIR spectra of untreated MP samples (black line), MPs pretreated with selected AOP (blue line) and MPs pretreated with AOP and subsequently biologically treated with *Candida parapsilosis* (red line). The cases presented are (**A**) PS MPs and (**B**) PVC MPs.

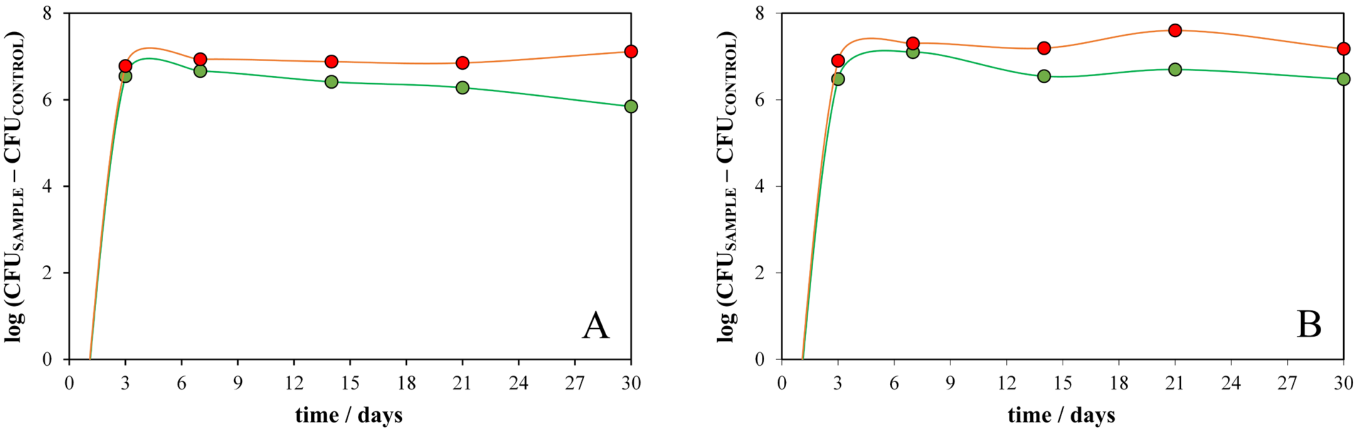

Figure 4. Comparison of CFU values determined during the biodegradation process of non-pretreated (green circles) and AOP-pretreated MP samples (orange circles). The cases shown are (**A**) PS samples and (**B**) PVC samples.

In the end, it seems important to say that *Candida parapsilosis*, the yeast used in this study, is a pathogen and one of the main causes of invasive candidal disease [75]. However, it is a microorganism that is not harmful to humans under normal circumstances, as it is commonly found on the skin, in the gastrointestinal tract and on mucous membranes [76].

The problem can only arise when this microorganism enters a wound. Therefore, the presence of biofilms of *Candida parapsilosis* on the plastic parts of medical equipment is still the main source of infection [77]. The fact that this microorganism can survive on the plastic parts of medical equipment can be seen as an additional argument that *Candida parapsilosis* is able to adapt to MPs.

4. Conclusions

In this study, we tested the applicability of UV-C/H_2O_2 and UV-C/$S_2O_8^{2-}$ AOPs as a pre-step for the biotreatment of PS and PVC MPs by the yeast culture *Candida parapsilosis* isolated from an MP-rich environment. The use of AOPs as a pretreatment implied a restrictive use of AOPs, e.g., to affect only the surface of the MPs, which would not be very costly but could be very beneficial for the efficiency of the biodegradation process. The AOPs mentioned were chosen due to their frequent use in solving a problem with various recalcitrant organic pollutants and due to the high oxidizing power of the radical species involved.

The influence of three process parameters on the efficiency of the applied AOPs in the degradation of MP samples was tested: the initial pH of the solution (tested in the range of 4–10), the initial concentration of peroxide used (1–20 mM) and the treatment duration (up to 90 min). The experimental design followed a full factorial methodology, with each parameter tested at three levels. The efficiency of degradation was evaluated by the relative change in intensity of the selected characteristic FTIR bands: out-of-plane C-H bending at 694.4 cm^{-1} for PS and CH_2 bending at 1411.9 cm^{-1} for PVC samples. Within the applied parameter range, both PS samples and PVC samples were found to be sensitive to the tested photochemical AOPs. A statistical analysis of the treatment results (i.e., the relative change in intensities of selected FTIR bands) confirmed the significant influence of all three tested parameters. The UV-C/H_2O_2 treatment was found to be more effective in degrading PS samples, with a slightly acidic environment, maximum peroxide concentration and maximum treatment duration, leading to the maximum degradation efficiency. For PVC samples, the UV-C/$S_2O_8^{2-}$ treatment led to better treatment results. The maximum efficiency was achieved in a slightly basic environment with a medium peroxide concentration (11.1 mM) for 90 min (maximum treatment duration). Generally speaking, the biodegradation of the pretreated samples resulted in a higher number of yeast cells in the biological treatment system compared to the biological treatment of the non-pretreated samples, indicating a positive effect of the pretreatment on PS and PVC MPs during biodegradation with the yeast *Candida parapsilosis*. The results imply that increasing the duration of the AOP pretreatment or adding more peroxide, as in the case of the UV-C/H_2O_2 treatment of PS MPs, would lead to greater MP degradation during the pretreatment step; this could improve the efficiency of the biological treatment. However, such changes require the delicate consideration of increasing costs (electricity costs, lamp costs and costs of chemicals for oxidation and pH adjustment), and a balance must be found between the increased treatment costs and increased efficiency.

As far as we know, this is the first study on the influence of an AOP pretreatment on the biodegradation of PS and PVC MPs by fungi and one of the few on the biodegradation of AOP-pretreated MPs samples in general. Considering the current societal trends aimed at sustainable development and green technologies, as well as the advantages characterizing treatments such as the one described in the study (high metabolic potential of fungi, very economical and environmentally friendly approach), an intensification of research on the biodegradation of MPs by fungal species is expected. This includes, among other things, a more detailed investigation of various pretreatments that could increase the effectiveness of the biological treatment.

Supplementary Materials: The following supporting information can be downloaded at: https://www.mdpi.com/article/10.3390/w16101389/s1, Figure S1: FTIR spectra of untreated MP samples with the characteristic bands indicated: (A) PS MPs and (B) PVC MPs. The chemical structures of the mentioned polymers are shown in blue; Table S1: Statistical analysis of the fitted response surface models (Equations (1)–(4)) for MPs treated with UV-C/H_2O_2 or UV-C/$S_2O_8{}^{2-}$. The analysis was performed with a significance of $p < 0.050$; Table S2: Estimated values of the coefficients of the RSM models selected as optimal for the applied AOP treatments (according to Equation (4)) and the results of the t-test presented in the form of p-values. The calculations were performed with a significance level of $p < 0.050$.

Author Contributions: Conceptualization, M.M. (Marinko Markić), Š.U. and D.K.G.; methodology, K.B.M., M.M. (Martina Miloloža) and M.C.; formal analysis, K.B.M. and V.M.; writing—original draft preparation, K.B.M.; writing—review and editing, Š.U. and D.K.G.; visualization, K.B.M. and Š.U; supervision, T.B. and M.U.B.; project administration, T.B. All authors have read and agreed to the published version of the manuscript.

Funding: The authors would like to acknowledge the financial support of the Croatian Science Foundation through the project Advanced Water Treatment Technologies for Microplastics Removal (AdWaTMiR; IP-2019-04-9661).

Data Availability Statement: Data are contained within the article.

Conflicts of Interest: The authors declare no conflicts of interest.

References

1. Eyerer, P.; Gettwert, V. Properties of Plastics in Structural Components. In *Polymers—Opportunities and Risks I*; Eyerer, P., Ed.; Springer: Berlin/Heidelberg, Germany, 2010; pp. 47–165. [CrossRef]
2. Lamichhane, G.; Acharya, A.; Marahatha, R.; Modi, B.; Paudel, R.; Adhikari, A.; Raut, B.K.; Aryal, S.; Parajuli, N. Microplastics in environment: Global concern, challenges, and controlling measures. *Int. J. Environ. Sci. Technol.* **2023**, *20*, 4673–4694. [CrossRef] [PubMed]
3. Amobonye, A.; Bhagwat, P.; Raveendran, S.; Singh, S.; Pillai, S. Environmental Impacts of Microplastics and Nanoplastics: A Current Overview. *Front. Microbiol.* **2021**, *12*, 768297. [CrossRef] [PubMed]
4. The 17 Goals. Available online: https://sdgs.un.org/goals (accessed on 26 April 2024).
5. Plastic Soup Foundation. Available online: https://www.plasticsoupfoundation.org/en/plastic-problem/sustainable-development/individual-sdgs/ (accessed on 26 April 2024).
6. Alqahtani, S.; Alqahtani, S.; Saquib, Q.; Mohiddin, F. Toxicological impact of microplastics and nanoplastics on humans: Understanding the mechanistic aspect of the interaction. *Front. Toxicol.* **2023**, *5*, 1193386. [CrossRef]
7. Zhao, H.; Hong, X.; Chai, J.; Wan, B.; Zhao, K.; Han, C.; Zhang, W.; Huan, H. Interaction between Microplastics and Pathogens in Subsurface System: What We Know So Far. *Water* **2024**, *16*, 499. [CrossRef]
8. Maddela, N.R.; Kakarla, D.; Venkateswarlu, K.; Megharaj, M. Additives of plastics: Entry into the environment and potential risks to human and ecological health. *J. Environ. Manag.* **2023**, *348*, 119364. [CrossRef] [PubMed]
9. Gao, W.; Zhang, Y.; Mo, A.; Jiang, J.; Liang, Y.; Cao, X.; He, D. Removal of microplastics in water: Technology progress and green strategies. *Green Anal. Chem.* **2022**, *3*, 100042. [CrossRef]
10. Nizzetto, L.; Futter, M.; Langaas, S. Are Agricultural Soils Dumps for Microplastics of Urban Origin? *Environ. Sci. Technol.* **2016**, *50*, 10777–10779. [CrossRef]
11. Iyare, P.U.; Ouki, S.K.; Bond, T. Microplastics removal in wastewater treatment plants: A critical review. *Environ. Sci. Water Res. Technol.* **2020**, *6*, 2664–2675. [CrossRef]
12. Ceretta, M.B.; Nercessian, D.; Wolski, E.A. Current Trends on Role of Biological Treatment in Integrated Treatment Technologies of Textile Wastewater. *Front. Microbiol.* **2021**, *12*, 651025. [CrossRef]
13. Okal, E.J.; Heng, G.; Magige, E.A.; Khan, S.; Wu, S.; Ge, Z.; Zhang, T.; Mortimer, P.E.; Xu, J. Insights into the mechanisms involved in the fungal degradation of plastics. *Ecotoxicol. Environ. Saf.* **2023**, *262*, 115202. [CrossRef]
14. Miri, S.; Saini, R.; Davoodi, S.M.; Pulicharla, R.; Brar, S.K.; Magdouli, S. Biodegradation of microplastics: Better late than never. *Chemosphere* **2022**, *286*, 131670. [CrossRef]
15. Lokesh, P.; Shobika, R.; Omer, S.; Reddy, M.; Saravanan, P.; Rajeshkannan, R.; Saravanan, V.; Venkatkumar, S. Bioremediation of plastics by the help of microbial tool: A way for control of plastic pollution. *Sustain. Chem. Environ.* **2023**, *3*, 100027. [CrossRef]
16. Cai, Z.; Li, M.; Zhu, Z.; Wang, X.; Huang, Y.; Li, T.; Gong, H.; Yan, M. Biological Degradation of Plastics and Microplastics: A Recent Perspective on Associated Mechanisms and Influencing Factors. *Microorganisms* **2023**, *11*, 1661. [CrossRef]
17. Ghosh, S.; Qureshi, A.; Purohit, H.J. Microbial Degradation of Plastics: Biofilms and Degradation Pathways. In *Contaminants in Agriculture and Environment: Health Risks and Remediation*; Kumar, V., Kumar, R., Singh, J., Kumar, P., Eds.; Agro Environ Media: Haridwar, India, 2019; pp. 184–199. [CrossRef]

18. Hanpanich, O.; Wongkongkatep, P.; Pongtharangkul, T.; Wongkongkatep, J. Turning hydrophilic bacteria into biorenewable hydrophobic material with potential antimicrobial activity via interaction with chitosan. *Bioresour. Technol.* **2017**, *230*, 97–102. [CrossRef] [PubMed]
19. Bayry, J.; Aimanianda, V.; Guijarro, J.I.; Sunde, M.; Latgé, J.-P. Hydrophobins—Unique Fungal Proteins. *PLoS Pathog.* **2012**, *8*, e1002700. [CrossRef]
20. Tokiwa, Y.; Calabia, B.P.; Ugwu, C.U.; Aiba, S. Biodegradability of plastics. *Int. J. Mol. Sci.* **2009**, *10*, 3722–3742. [CrossRef]
21. Du, H.; Xie, Y.; Wang, J. Microplastic degradation methods and corresponding degradation mechanism: Research status and future perspectives. *J. Hazard. Mater.* **2021**, *418*, 126377. [CrossRef] [PubMed]
22. Hamd, W.; Daher, E.A.; Tofa, T.S.; Dutta, J. Recent Advances in Photocatalytic Removal of Microplastics: Mechanisms, Kinetic Degradation, and Reactor Design. *Front. Mar. Sci.* **2022**, *9*, 885614. [CrossRef]
23. Mousset, E.; Loh, W.H.; Lim, W.S.; Jarry, L.; Wang, Z.; Lefebvre, O. Cost comparison of advanced oxidation processes for wastewater treatment using accumulated oxygen-equivalent criteria. *Water Res.* **2021**, *200*, 117234. [CrossRef]
24. Rodríguez, M. Fenton and UV-Vis Based Advanced Oxidation Processes in Wastewater Treatment: Degradation, Mineralization and Biodegradability Enhancement. Ph.D. Thesis, University of Barcelona, Faculty of Chemistry, Barcelona, Spain, 2003.
25. Armstrong, D.A.; Huie, R.E.; Koppenol, W.H.; Lymar, S.V.; Merényi, G.; Neta, P.; Ruscic, B.; Stanbury, D.M.; Steenken, S.; Wardman, P. Standard electrode potentials involving radicals in aqueous solution: Inorganic radicals (IUPAC Technical Report). *Pure Appl. Chem.* **2015**, *87*, 1139–1150. [CrossRef]
26. Cheng, M.; Zeng, G.; Huang, D.; Lai, C.; Xu, P.; Zhang, C.; Liu, Y. Hydroxyl radicals based advanced oxidation processes (AOPs) for remediation of soils contaminated with organic compounds: A review. *Chem. Eng. J.* **2016**, *284*, 582–598. [CrossRef]
27. Wang, J.L.; Xu, L.J. Advanced Oxidation Processes for Wastewater Treatment: Formation of Hydroxyl Radical and Application. *Environ. Sci. Technol.* **2012**, *42*, 251–325. [CrossRef]
28. Zoschke, K.; Dietrich, N.; Börnick, H.; Worch, E. UV-based advanced oxidation processes for the treatment of odour compounds: Efficiency and by-product formation. *Water Res.* **2012**, *46*, 5365–5373. [CrossRef] [PubMed]
29. Cataldo, F. Hydrogen peroxide photolysis with different UV light sources including a new UV-LED light source. *New Front. Chem.* **2014**, *23*, 99–110.
30. Aye, T.T.; Low, T.Y.; Sze, S.K. Nanosecond laser-induced photochemical oxidation method for protein surface mapping with mass spectrometry. *Anal Chem.* **2005**, *77*, 5814–5822. [CrossRef] [PubMed]
31. Urbina-Suarez, N.A.; López-Barrera, G.L.; García-Martínez, J.B.; Barajas-Solano, A.F.; Machuca-Martínez, F.; Zuorro, A. Enhanced UV/H_2O_2 System for the Oxidation of Organic Contaminants and Ammonia Transformation from Tannery Effluents. *Processes* **2023**, *11*, 3091. [CrossRef]
32. Račytė, J.; Rimeika, M. Factors influencing efficiency of UV/H_2O_2 advanced oxidation process. In *2007: Proceedings from Kalmar ECO-TECH'07: Technologies for Waste and Wastewater Treatment, Energy from Wast, Remediation of Contaminated Sited, Emissions Related to Climate, Kalmar, Sweden, 26–28 November 2007*; Kaczala, F., Hogland, W., Marques, M., Vinrot, E., Eds.; Linnaeus University: Växjö, Sweden, 2007; pp. 757–769. [CrossRef]
33. Zhou, C.; Gao, N.; Deng, Y.; Chu, W.; Rong, W.; Zhou, S. Factors affecting ultraviolet irradiation/hydrogen peroxide (UV/H_2O_2) degradation of mixed N-nitrosamines in water. *J. Hazard. Mater.* **2012**, *43*, 231–232. [CrossRef] [PubMed]
34. Lopez-Alvarez, B.; Villegas-Guzman, P.; Peñuela, G.A.; Torres-Palma, R.A. Degradation of a Toxic Mixture of the Pesticides Carbofuran and Iprodione by UV/H_2O_2: Evaluation of Parameters and Implications of the Degradation Pathways on the Synergistic Effects. *Water Air Soil Pollut.* **2016**, *227*, 215. [CrossRef]
35. Guerra-Rodríguez, S.; Rodríguez, E.; Singh, D.; Rodríguez-Chueca, J. Assessment of Sulfate Radical-Based Advanced Oxidation Processes for Water and Wastewater Treatment: A Review. *Water* **2018**, *10*, 1828. [CrossRef]
36. Xia, X.; Zhu, F.; Li, J.; Yang, H.; Wei, L.; Li, Q.; Jiang, J.; Zhang, G.; Zhao, Q. A Review Study on Sulfate-Radical-Based Advanced Oxidation Processes for Domestic/Industrial Wastewater Treatment: Degradation, Efficiency, and Mechanism. *Front. Chem.* **2020**, *8*, 592056. [CrossRef]
37. Moreno-Andrés, J.; Rueda-Márquez, J.J.; Homola, T.; Vielma, J.; Moríñigo, M.Á.; Mikola, A.; Sillanpää, M.; Acevedo-Merino, A.; Nebot, E.; Levchuk, I. A comparison of photolytic, photochemical and photocatalytic processes for disinfection of recirculation aquaculture systems (RAS) streams. *Water Res.* **2020**, *181*, 115928. [CrossRef] [PubMed]
38. Hüffer, T.; Weniger, A.-K.; Hofmann, T. Sorption of organic compounds by aged polystyrene microplastic particles. *Environ. Pollut.* **2018**, *236*, 218–225. [CrossRef] [PubMed]
39. Dong, S.; Yan, X.; Yue, Y.; Li, W.; Luo, W.; Wang, Y.; Sun, J.; Li, Y.; Liu, M.; Fan, M. H_2O_2 concentration influenced the photoaging mechanism and kinetics of polystyrene microplastic under UV irradiation: Direct and indirect photolysis. *J. Clean. Prod.* **2022**, *380*, 135046. [CrossRef]
40. Hankett, J.M.; Welle, A.; Lahann, J.; Chen, Z. Evaluating UV/H_2O_2 Exposure as a DEHP Degradation Treatment for Plasticized PVC. *J. Appl. Polym. Sci.* **2014**, *131*, 40649. [CrossRef]
41. Hankett, J.M.; Collin, W.R.; Chen, Z. Molecular Structural Changes of Plasticized PVC after UV Light Exposure. *J. Phys. Chem. B* **2013**, *117*, 16336–16344. [CrossRef] [PubMed]
42. Liu, P.; Qian, L.; Wang, H.; Zhan, X.; Lu, K.; Gu, C.; Gao, S. New insights into the aging behavior of microplastics accelerated by advanced oxidation processes. *Environ. Sci. Technol.* **2019**, *53*, 3579–3588. [CrossRef] [PubMed]

43. Zhang, Y.; Jiang, H.; Wang, H.; Wang, C. Separation of hazardous polyvinyl chloride from waste plastics by flotation assisted with surface modification of ammonium persulfate: Process and mechanism. *J. Hazard. Mater.* **2020**, *389*, 121918. [CrossRef] [PubMed]
44. El-Gendi, H.; Saleh, A.K.; Badierah, R.; Redwan, E.M.; El-Maradny, Y.A.; El-Fakharany, E.M. A Comprehensive Insight into Fungal Enzymes: Structure, Classification, and Their Role in Mankind's Challenges. *J. Fungi* **2021**, *8*, 23. [CrossRef] [PubMed]
45. Gangola, S.; Joshi, S.; Kumar, S.; Pandey, S.C. Chapter 10—Comparative Analysis of Fungal and Bacterial Enzymes in Biodegradation of Xenobiotic Compounds. In *Smart Bioremediation Technologies*; Bhatt, P., Ed.; Academic Press: Chennai, India, 2019; pp. 169–189. [CrossRef]
46. Harding, M.W.; Marques, L.L.R.; Howard, R.J.; Olson, M.E. Can filamentous fungi form biofilms? *Trends Microbiol.* **2009**, *17*, 475–480. [CrossRef] [PubMed]
47. Bule Možar, K.; Miloloža, M.; Martinjak, V.; Cvetnić, M.; Ocelić Bulatović, V.; Mandić, V.; Bafti, A.; Ukić, Š.; Kučić Grgić, D.; Bolanča, T. Bacteria and Yeasts Isolated from the Environment in Biodegradation of PS and PVC Microplastics: Screening and Treatment Optimization. *Environments* **2023**, *10*, 207. [CrossRef]
48. Hock, O.G.; Lum, H.W.; De Qin, D.; Kee, W.K.; Shing, W.L. The growth and laccase activity of edible mushrooms involved in plastics degradation. *Curr. Top. Toxicol.* **2019**, *15*, 57–62.
49. Atiq, N. Biodegradability of Synthetic Plastics Polystyrene and Styrofoam by Fungal Isolates. Ph.D. Thesis, Quaid-i-Azam University, Islamabad, Pakistan, 2011.
50. Chaudhary, A.K.; Vijayakumar, R.P. Studies on biological degradation of polystyrene by pure fungal cultures. *Environ. Dev. Sustain.* **2020**, *22*, 4495–4508. [CrossRef]
51. Chaudhary, A.K.; Chaitanya, K.; Vijayakumar, R.P. Synergistic effect of UV and chemical treatment on biological degradation of Polystyrene by *Cephalosporium* strain NCIM 1251. *Arch. Microbiol.* **2021**, *203*, 2183–2191. [CrossRef]
52. Motta, O.; Proto, A.; De Carlo, F.; De Caro, F.; Santoro, E.; Brunetti, L.; Capunzo, M. Utilization of chemically oxidized polystyrene as co-substrate by filamentous fungi. *Int. J. Hyg. Environ. Health* **2009**, *212*, 61–66. [CrossRef]
53. Galgali, P. Fungal degradation of carbohydrate-linked polystyrenes. *Carbohydr. Polym.* **2004**, *55*, 393–399. [CrossRef]
54. Srikanth, M.; Sandeep, T.S.R.S.; Sucharitha, K.; Godi, S. Biodegradation of plastic polymers by fungi: A brief review. *Bioresour. Bioprocess.* **2022**, *9*, 42. [CrossRef]
55. Ekanayaka, A.H.; Tibpromma, S.; Dai, D.; Xu, R.; Suwannarach, N.; Stephenson, S.L.; Dao, C.; Karunarathna, S.C. A Review of the Fungi That Degrade Plastic. *J. Fungi* **2022**, *8*, 772. [CrossRef]
56. Sakhalkar, S.; Mishra, R. Screening and Identification of Soil Fungi with Potential of Plastic Degrading Ability. *Indian J. Appl. Res.* **2013**, *3*, 62–64. [CrossRef]
57. Malachová, K.; Novotný, Č.; Adamus, G.; Lotti, N.; Rybková, Z.; Soccio, M.; Šlosarčíková, P.; Verney, V.; Fava, F. Ability of *Trichoderma hamatum* Isolated from Plastics-Polluted Environments to Attack Petroleum-Based, Synthetic Polymer Films. *Processes* **2020**, *8*, 467. [CrossRef]
58. Sumathi, T.; Viswanath, B.; Sri Lakshmi, A.; SaiGopal, D.V.R. Production of Laccase by *Cochliobolus* sp. Isolated from Plastic Dumped Soils and Their Ability to Degrade Low Molecular Weight PVC. *Biochem. Res. Int.* **2016**, *2016*, 1–10. [CrossRef] [PubMed]
59. Kirbaş, Z.; Keskin, N.; Güner, A. Biodegradation of polyvinylchloride (PVC) by white rot fungi. *Bull. Environ. Contam. Toxicol.* **1999**, *63*, 335–342. [CrossRef]
60. Ali, M.I.; Ahmed, S.; Robson, G.; Javed, I.; Ali, N.; Atiq, N.; Hameed, A. Isolation and molecular characterization of polyvinyl chloride (PVC) plastic degrading fungal isolates. *J. Basic Microbiol.* **2013**, *54*, 18–27. [CrossRef]
61. Webb, J.S.; Nixon, M.; Eastwood, I.M.; Greenhalgh, M.; Robson, G.D.; Handley, P.S. Fungal Colonization and Biodeterioration of Plasticized Polyvinyl Chloride. *Appl. Environ. Microbiol.* **2000**, *66*, 3194–3200. [CrossRef]
62. Gómez-Méndez, L.D.; Moreno-Bayona, D.A.; Poutou-Piñales, R.A.; Salcedo-Reyes, J.C.; Pedroza-Rodríguez, A.M.; Vargas, A.; Bogoya, J.M. Biodeterioration of plasma pretreated LDPE sheets by *Pleurotus ostreatus*. *PLoS ONE* **2018**, *13*, e0203786. [CrossRef]
63. Scally, L.; Gulan, M.; Weigang, L.; Cullen, P.J.; Milosavljevic, V. Significance of a Non-Thermal Plasma Treatment on LDPE Biodegradation with *Pseudomonas aeruginosa*. *Materials* **2018**, *11*, 1925. [CrossRef]
64. Jeyakumar, D.; Chirsteen, J.; Mukesh, D. Synergistic effects of pretreatment and blending on fungi mediated biodegradation of polypropylenes. *Bioresour. Technol.* **2013**, *148*, 78–85. [CrossRef]
65. Tribedi, P.; Dey, S. Pre-oxidation of low-density polyethylene (LDPE) by ultraviolet light (UV) promotes enhanced degradation of LDPE in soil. *Environ. Monit. Assess.* **2017**, *189*, 624. [CrossRef]
66. Fang, J.; Xuan, Y.; Li, Q. Preparation of polystyrene spheres in different particle sizes and assembly of the PS colloidal crystals. *Sci. China Technol. Sci.* **2010**, *53*, 3088–3093. [CrossRef]
67. Amar, Z.H.; Chabira, S.F.; Sebaa, M.; Ahmed, B. Structural changes undergone during thermal aging and/or processing of unstabilized, dry-blend and rigid PVC, investigated by FTIR-ATR and curve fitting. *Ann. Chim. Sci. Mater.* **2019**, *43*, 59–68. [CrossRef]
68. Gong, Y.; Ding, P.; Xu, M.-J.; Zhang, C.-M.; Xing, K.; Qin, S. Biodegradation of phenol by a halotolerant versatile yeast *Candida tropicalis* SDP-1 in wastewater and soil under high salinity conditions. *J. Environ. Manag.* **2021**, *289*, 112525. [CrossRef] [PubMed]
69. Black, J.G. *Microbiology: Principles and Explorations*, 8th ed.; John Wiley & Sons: Hoboken, NJ, USA, 2012; p. 975.
70. Liu, X. *Organic Chemistry I*; Kwantlen Polytechnic University: Surrey, BC, Canada, 2021; p. 198.
71. Herrera-Ordonez, J. The role of sulfate radicals and pH in the decomposition of persulfate in aqueous medium: A step towards prediction. *Chem. Eng. J. Adv.* **2022**, *11*, 100331. [CrossRef]

72. Honarmandrad, Z.; Sun, X.; Wang, Z.; Naushad, M.; Boczkaj, G. Activated persulfate and peroxymonosulfate based advanced oxidation processes (AOPs) for antibiotics degradation—A review. *Water Resour. Ind.* **2023**, *29*, 100194. [CrossRef]
73. Mahbobi, M.; Tiemann, T.K. Chapter 8. Regression Basics. In *Introductory Business Statistics with Interactive Spreadsheets—1st Canadian Edition*, 1st ed.; Mahbobi, M., Tiemann, T.K., Eds.; Pressbooks: Montreal, QC, Canada; Available online: https://opentextbc.ca/introductorybusinessstatistics/chapter/regression-basics-2/ (accessed on 28 February 2024).
74. Frost, J. Statistics By Jim. T-Distribution Table of Critical Values. Available online: https://statisticsbyjim.com/hypothesis-testing/t-distribution-table/ (accessed on 28 February 2024).
75. Trofa, D.; Gácser, A.; Nosanchuk, J.D. *Candida parapsilosis*, an emerging fungal pathogen. *Clin. Microbiol. Rev.* **2008**, *21*, 606–625. [CrossRef]
76. Branco, J.; Miranda, I.M.; Rodrigues, A.G. *Candida parapsilosis* Virulence and Antifungal Resistance Mechanisms: A Comprehensive Review of Key Determinants. *J. Fungi* **2023**, *9*, 80. [CrossRef]
77. Tóth, R.; Nosek, J.; Mora-Montes, H.M.; Gabaldon, T.; Bliss, J.M.; Nosanchuk, J.D.; Turner, S.A.; Butler, G.; Vágvölgyi, C.; Gácser, A. *Candida parapsilosis*: From Genes to the Bedside. *Clin. Microbiol. Rev.* **2019**, *32*, e00111-18. [CrossRef]